Shape-Dependent Photocatalysis

DOI: 10.1002/ange.201108580

Shape-Dependent Acidity and Photocatalytic Activity of Nb_2O_5 Nanocrystals with an Active TT (001) Surface

*Yun Zhao, Clive Eley, Jingping Hu, John S Foord, Lin Ye, Heyong He, and Shik Chi Edman Tsang**

The search for new low carbon and clean energy technologies is prominent on the research agendas of many governments, universities, and industrial sectors. In particular, the possibility of using solar energy for hydrogen production, fine chemicals manufacture, and water cleansing is currently under intense research. The use of semiconducting oxides, such as TiO_2 and ZnO, as photoactive materials has been receiving much attention. Recent work indicates that nanoparticles of these compounds show strong shape-dependent (surface-dependent) photocatalytic properties.[1,2] Spherical nanoparticles with high specific surface area to volume ratios are generally preferred. However, the high electron–hole recombination rate sometimes seen on their defect-rich nonplanar surfaces can be problematic.[1] As an n-type transition metal oxide semiconductor, Nb_2O_5 has attracted a great deal of interest owing to remarkable applications in gas sensing, acid catalysis, electrochromics, field emission displays, and microelectronics.[3–7] Despite having high photocatalytic activity and well-documented water-tolerant acidic surfaces, at present there are few studies concerning the use of Nb_2O_5-based materials for photocatalytic applications.[8,9] Herein we report that the (100) surface lying along the axis of pseudo-hexagonal TT Nb_2O_5 nanorod crystals offers enhanced photocatalytic activity over nanospheres for methylene blue decomposition in aqueous solution. We also reveal for the first time that the strong acidic sites on the exposed crystallographic planes of the nanorods readily bind methylene blue molecules from solution. In the presence of a typical radical scavenger (DMSO), Nb_2O_5 nanorods show only a marginal decrease in decomposition rate. This is in contrast to ZnO, which adopts the classical mechanism of hole-induced hydroxyl radical attack on organic molecules in solution. The unique combination of adsorption and preconcentration of organic contaminants followed by direct surface decomposition driven by photocarriers gives rise to improved efficiency in this nonclassical mechanism for photomineralization on a Nb_2O_5 surface.

[*] Y. Zhao, C. Eley, J. Hu, J. S. Foord, Prof. S. C. E. Tsang
Wolfson Catalysis Centre, Department of Chemistry, University of Oxford, Oxford, OX1 3QR (UK)
E-mail: edman.tsang@chem.ox.ac.uk
Y. Zhao
School of Chemical Engineering and Environment, Beijing Institute of Technology (P.R. China)
L. Ye, H. He
Department of Chemistry, Fudan University, Shanghai (P.R. China)

Supporting information for this article is available on the WWW under http://dx.doi.org/10.1002/anie.201108580.

Details on materials synthesis, testing, and characterization can be found in the Supporting Information. As seen from the TEM image in Figure 1 a, Nb_2O_5 nanospheres of 20–50 nm diameter were obtained by our precipitation method. Selected area electron diffraction (SAED) (see the Supporting Information) gave ring patterns indicative of the poor long-range crystallinity of the Nb_2O_5 nanospheres. This is not surprising given the fact that the rapid non-equilibrium precipitation conditions do not allow for the extended growth of a particular phase. Thus, spherically shaped particles that offer a decrease in overall surface energy are anticipated. However, in the case of Nb_2O_5 nanorod synthesis, we employed the solvothermal technique over a lengthy growth period in the presence of a structure-directing agent, oleic acid in trioctylamine. The TEM image in Figure 1 b clearly shows the formation of rod structures (stacked bundles) with sharp edges indicative of small single crystals. As shown, the rod length ranges from 100 to 500 nm with a diameter of 5–20 nm. Indeed, the SAED (see the Supporting Information) shows a single diffraction pattern. The lattice parameters, calculated with the camera constant of the microscope taken into account, matched with the pseudohexagonal TT structure of the Nb_2O_5 phase. A HRTEM study of many randomly selected Nb_2O_5 nanorod bundles clearly showed lattice fringes perpendicular to the rod axis, and the fringe separation of 3.9 ± 0.3 Å corresponds closely to the (001) crystal plane with the predominant (001) exposed on the bundle surfaces (Figure 1 c). Thus, the crystal growth of the nanorod appears to follow the [001] zone direction in the presence of the organic directing agent. It is known that oleic acid can form lamella rod-like structures in amine solution,[10] in which ammonium niobate oxalate is partially soluble. This allows for the careful control of dissolution, hydrolysis, and recrystallization processes to template the growth of nanorod

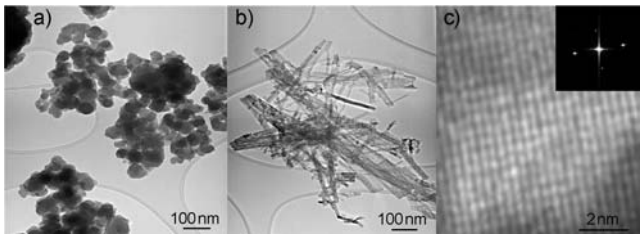

Figure 1. Analysis of Nb_2O_5 nanostructures. a) TEM image of Nb_2O_5 nanospheres; b) TEM image of Nb_2O_5 nanorods; c) HRTEM image and electron diffraction of Nb_2O_5 nanorods showing the [001] zone axis with a (001) fringe separation of 3.9 ± 0.3 Å along the rod surface.

single crystals. XRD suggests that both the nanospheres and nanorods adopt the pseudohexagonal TT phase, however a poorer crystallinity (short-range order) with lower intensity of peaks for the Nb_2O_5 nanospheres is evident (see the Supporting Information). The enhancement in (001) peak intensity relative to the typical powder diffraction pattern is caused by the preferred orientation of Nb_2O_5 rod crystals.

Photocatalytic decomposition of methylene blue in an aqueous solution was evaluated in the presence of Nb_2O_5 spheres or rods and compared to ZnO plates under ultraviolet irradiation. As seen from Figure 2 (see also the Supporting Information), the reaction, monitored at 664.5 nm (corresponding to monomer absorption), followed pseudo-first order reaction kinetics for the two forms of Nb_2O_5. The apparent rate constant was calculated to be $k = 0.0733\ min^{-1}$ for the rods and $0.0074\ min^{-1}$ for the spheres (see the Supporting Information). Thus, the rate constant for the rods was almost 10 times higher than that of the spheres as well as being more active than the ZnO plates (see the Supporting Information). Saito and Kudo reported enhanced photocatalytic activities for H_2 evolution from water by photocatalytic decomposition using TT Nb_2O_5 nanowires (vs. spherical particles) with a similar morphology to our rods.[11] They suggested that one possibility is the difference in the surface area of the wires versus the spheres. However, the measured N_2 BET surface areas for our spheres and rods were 77.27 and 102.99 $m^2 g^{-1}$, respectively. The small difference in the specific surface area between them implies that surface structure and electronic properties, rather than surface area, are the key factors for the observed high decomposition rates.

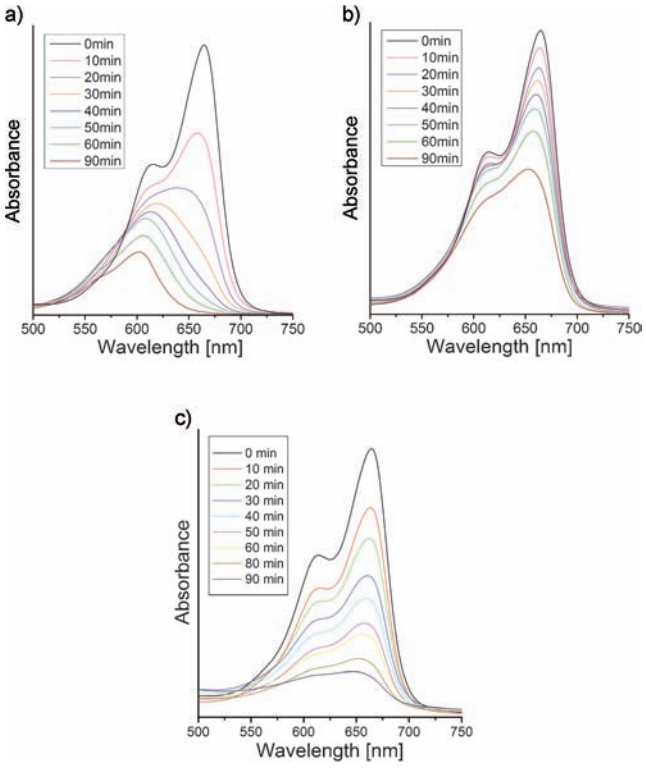

Figure 2. UV/Vis absorption curves of methylene blue versus UV irradiation time with: a) Nb_2O_5 nanorods, b) Nb_2O_5 nanospheres, and c) ZnO nanoplates.

Diffuse reflectance UV–visible spectra showed different absorption edges for Nb_2O_5 rods and spheres (see the Supporting Information) compared to the bulk band gap (E_g), which is size dependent.[12] The apparently higher E_g of the spheres may be accounted for by the lower number of interconnected Nb–O polyhedra,[12] which was also reflected in the poor crystallinity shown by SAED and XRD analysis. It is important to note the longer absorption tail stretching to the visible region for the spheres (see the Supporting Information), which indicates a significant absorption range adjacent to the interband transition because of the presence of defects. XPS confirmed that the rods gave a surface stoichiometric Nb/O ratio and binding energy (BE) comparable to bulk Nb_2O_5 crystals. However, there were significant BE shifts for Nb 3d 5/2 and O 1s peaks for the spheres. These variations are ascribed to the formation of oxygen vacancies $V_{O^{2+}}$ with reduction of Nb^{5+} to Nb^{4+} on the surface.

The surface of Nb_2O_5 is known to be covered with acidic sites[8–10,12,13] comparable to the strength of 70% sulphuric acid ($H_0 = -5.6$). Thus, the difference in the nature of these Lewis acid sites may account for the observed photocatalytic differences between spheres and rods. Infrared spectra of Nb_2O_5 spheres and rods were recorded using adsorbed pyridine at different desorption temperatures.[14] IR bands at 1450 cm^{-1} and 1550 cm^{-1} can be attributed to pyridine coordinated to a Lewis acid site and pyridinium on Brønsted acid sites, respectively.[14] There was only one peak at 1450 cm^{-1}, indicating that both spheres and rods contained only Lewis acid sites after calcination. Based on the temperature programmed desorption peak areas, we estimated that there were nearly three times as many Lewis acid sites on the rods as on the spheres. The surface hydrolysis of Nb^{5+}–O may also contribute to strong Brønsted acidity, thus rendering the rod surfaces much more acidic. The nucleophilic moieties of methylene blue, such as lone pair electrons in nitrogen and sulfur may adsorb on these strongly Lewis acidic Nb^{5+} sites before irradiation. To test this, the degree of adsorption on the nanorods was assessed in the absence of a light source. The nanorods indeed exhibited a strong affinity for the dye molecules, particularly binding methylene blue monomers (absorption at 664.5 nm; uptake of 4.11×10^{18} molecules per gram of rods) from solution in preference to the dimers (absorption at 620 nm), with absorption profiles similar to Figure 2a in the presence of light. However, fewer dye molecules were observed to adsorb on ZnO. IR spectra were collected for adsorbed dye species on the surface of Nb_2O_5 nanorods after a gentle rinse with water (see the Supporting Information). Without discussing in detail the assignment of individual peaks, it was seen that the number of peaks of adsorbed methylene blue compared to the free molecules decreased. This observation can be attributed to the disruption of flexional degrees of freedom when the molecule is in an adsorbed state, which suggests a strong chemical interaction.

In the classical mechanism for photoirradiation of n-type semiconductor oxides, excitons and unbound charge carriers are generated. Hydroxyl radicals can be produced when these excitations migrate to the surface and react with adsorbed water molecules or hydroxide ions. When released, these

radicals cause decomposition of organic molecules, such as dye molecules, in the solution phase. Thus, the photoactivity of ZnO is known to be reduced in the presence of a radical scavenger, such as dimethyl sulfoxide (DMSO).[15] Figure 3a shows about a two-fold rate attenuation when DMSO is added to a methylene blue solution containing the ZnO nanoplates (see the Supporting Information). On the other hand, Figure 3b shows an unexpected increase in the concentration of the dye molecules in solution with the Nb_2O_5 nanorods during the first 10 mins. It was thought that the added DMSO might change the dielectric constant of the solution, thus altering the partition and releasing some adsorbed species into the solution under irradiation conditions. There is also the possibility that some DMSO molecules may selectively bind to the acidic sites, thus causing dye displacement in a dynamic equilibria with their free forms in solution. After the initial increase in the dye concentration in solution, the rate of decomposition (slope of the curve) was almost comparable to that of Nb_2O_5 rods in the absence of DMSO, indicating that the radical scavenger had only a marginal effect on photocatalysis (see the Supporting Information). With regards to the strong adsorption of the dye molecules (UV/Vis and IR results) it appears that the dye species is immobilized by the solid acid sites where the photoinduced electrons and holes on the surface can attack them without recourse to the classical radical mechanism. The rate of attack for the monomers is clearly higher than that of the dimers, as can be seen in Figure 2a and b, where the 664.5 nm peak decreases much faster than the 620 nm peak, as the surface affinity for the monomer on the rods is stronger than the monomer–monomer (dimer) interaction. This is in sharp contrast to the indiscriminate attack by radicals on both monomers and dimers in solution with the ZnO plates (Figure 2c). Related observations describing the preferential adsorption of methylene blue monomers over dimers using acidic clays have been made.[16] Thus, the purely surface events in the non-classical mechanism over the acidic Nb_2O_5 rod-shaped crystals can account for the insensitivity towards radical scavengers added to the solution (see Figure 4).

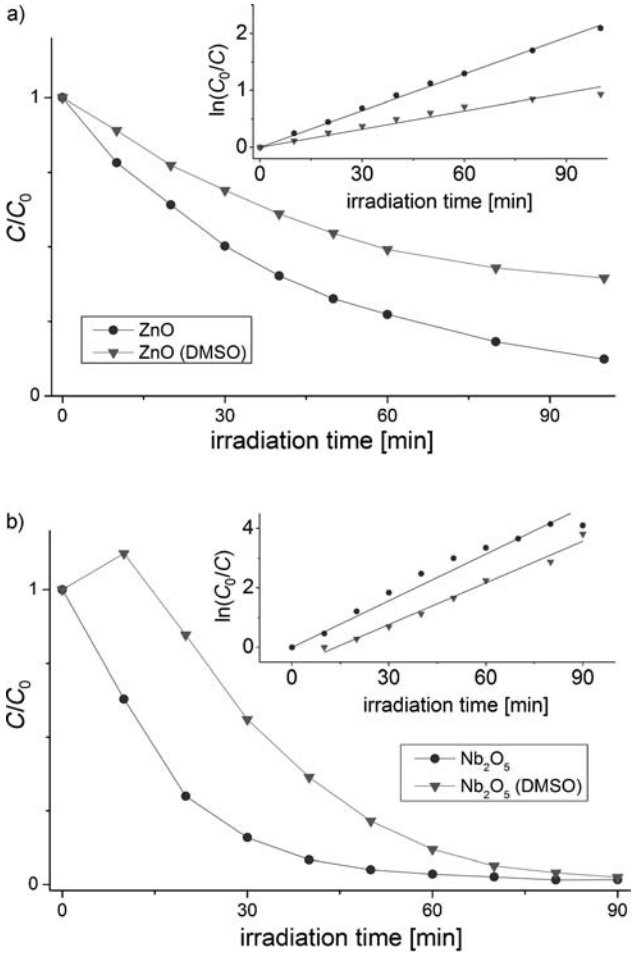

Figure 3. Photocatalytic activity of nanostructures as indicated by methylene blue concentration versus UV irradiation time. a) ZnO nanoplates with DMSO (triangles) and without DMSO (circles); b) Nb_2O_5 nanorods with DMSO (triangles) and without DMSO (circles).

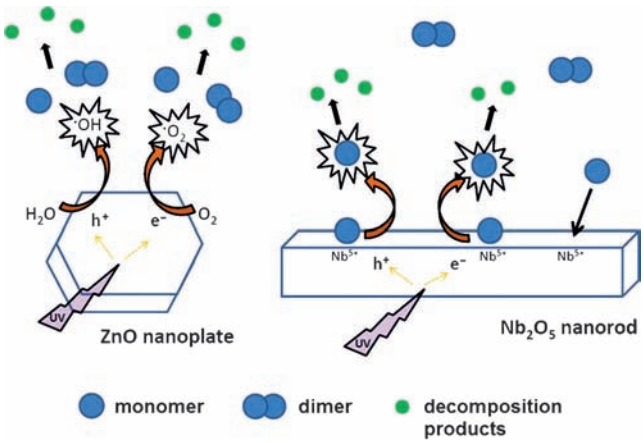

Figure 4. Models showing the classical radical attack by a ZnO nanoplate on monomers and dimers of methylene blue molecules in solution as compared to the non-classical excitons attack by an acidic Nb_2O_5 nanorod on adsorbed monomers.

To summarize, the strong Lewis acid sites on the TT Nb_2O_5 (001) surface can bind organic molecules from solution at locally high concentrations to provide a reservoir for more efficient photomineralization during irradiation, which accounts for the highest rate of photodecomposition observed in the present study. The shape-dependent acidic and photocatalytic properties are hereby described. These findings will further increase interest in the unique catalytic and photocatalytic properties of Nb_2O_5.[17,18]

Experimental Section

A precipitation reaction followed by calcination at 853 K was used to synthesize Nb_2O_5 nanospheres. Ammonium niobate oxylate hydrate (2.0 g; 99.99%, Aldrich) precursor was dissolved in distilled water (20 mL). The pH value of the solution was then adjusted to 9.0 by adding an ammonia solution with vigorous stirring. The white precipitate was separated by centrifugation and washed thoroughly with distilled water. Nb_2O_5 nanospheres were obtained by calcination of the dried precipitate at 853 K for 1 h. In a typical synthesis of

Nb_2O_5 nanorods, ammonium niobate oxylate hydrate (1.933 g, 6.38 mmol) was mixed with technical grade oleic acid (4 mL, 3.6 g, 12.76 mmol; 90%, Aldrich) in a 1:2 molar ratio, in trioctylamine (27 mL, 21.6 g, 61.07 mmol; 98%, Aldrich). The mixture was transferred into a 45 mL Teflon-lined autoclave and then heated hydrothermally at 453 K for 2–6 h. The white precipitate was collected by centrifugation and washed repeatedly with ethanol and acetone. Nb_2O_5 nanorods were obtained by calcination of the dried precipitate at 853 K for 1 h. A related synthetic method that produced poorly crystallized nanorods can be found in the literature.[19] The ZnO nanoplates were prepared according to the method published by McLaren et al.[2] using a 3:1 oleic acid to zinc ratio (zinc acetate, 99.5%, BDH). Methylene blue (> 99%, Aldrich) was used as a model organic contaminant. For comparison of the photocatalytic activity of Nb_2O_5 nanospheres and nanorods in Figure 2a and b, catalyst (60 mg) was dispersed in an aqueous methylene blue solution (60 mL, 15 mg L^{-1}). For the DMSO experiments presented in Figure 3 and Supporting Information Table 1, ZnO plates, Nb_2O_5 rods, or Nb_2O_5 spheres (13.5 mg) were added to an aqueous methylene blue solution (20 mL, 11.2 mg L^{-1}) with or without adding DMSO (0.215 mL; 99% Fischer; this amount is more than enough to cover the monolayer of all nanoparticles). The mixtures were magnetically stirred in the dark for 35 min before the reaction to encourage even dispersion of the nanoparticles and to establish an absorption/desorption equilibrium. The photocatalytic reaction was conducted at room temperature, with constant magnetic stirring to ensure full suspension of the particles throughout. The reaction took place in a Luzchem photoreactor, fitted with eight UVA tubes, and with radiation centered at 350 nm. The typical intensity inside the chamber was 0.3 mW cm^{-2}. Each reaction was conducted for 1.5 h, with 2–5 mL aliquots of reaction mixture extracted at 10 min intervals. These aliquots were centrifuged for 20 min at 8000 rpm prior to UV/Vis measurements to remove any suspended solid. A PerkinElmer LAMBDA 19 UV/Vis/NIR spectrometer was used to follow the decomposition of methylene blue. Absorption measurements were taken at 664.5 nm, as initial scans showed this to be the maximum absorbance wavelength for relevant concentrations of the dye. Concentrations were then determined by comparison to a calibration curve. The apparent rate constant values k were derived from the pseudo-first-order plots of each sample.

Received: December 6, 2011
Published online: February 1, 2012

Keywords: decomposition · Lewis acids · methylene blue · nanomaterials · photocatalysis

[1] N. Wu, J. Wang, D. N. Tafen, H. Wang, J.-G. Zheng, J. P. Lewis, X. Liu, S. S. Leonard, A. Manivannan, *J. Am. Chem. Soc.* **2010**, *132*, 6679 – 6685.
[2] A. Mclaren, T. Valdes-Solis, G. Li, S. C. Tsang, *J. Am. Chem. Soc.* **2009**, *131*, 12540 – 12541.
[3] Y. D. Wang, L. F. Yang, Z. L. Zhou, Y. F. Li, X. H. Wu, *Mater. Lett.* **2001**, *49*, 277 – 281.
[4] P. Carniti, A. Gervasini, M. Marzo, *J. Phys. Chem. C* **2008**, *112*, 14064 – 14074.
[5] S. H. Mujawar, A. I. Inamdar, S. B. Patil, P. S. Patil, *Solid State Ionics* **2006**, *177*, 3333 – 3338.
[6] R. Jose, V. Thavasi, S. Ramakrishna, *J. Am. Ceram. Soc.* **2009**, *92*, 289 – 301.
[7] K. S. Ahn, M. S. Kang, J. K. Lee, B. C. Shin, J. W. Lee, *Appl. Phys. Lett.* **2006**, *89*, 013103.
[8] G. S. Alexandre, L. B. Prado, C. P. Bolzon, A. O. Pedroso, L. L. C. Moura, *Appl. Catal. B* **2008**, *82*, 219 – 224.
[9] J. Wu, J. Li, X. Lü, L. Zhang, J. Yao, F. Zhang, F. Huang, F. Xu, *J. Mater. Chem.* **2010**, *20*, 1942 – 1946.
[10] Y. Q. Huang, Y. Lin, G. Zeng, Z. X. Liang, X. L. Liu, X. L. Hong, G. Y. Zhang, S. C. Tsang, *J. Mater. Chem.* **2008**, *18*, 5445 – 5447.
[11] K. Saito, A. Kudo, *Bull. Chem. Soc. Jpn.* **2009**, *82*, 1030 – 1034.
[12] R. Brayner, F. Bozon-Verduraz, *Phys. Chem. Chem. Phys.* **2003**, *5*, 1457 – 1466.
[13] K. Nakajima, Y. Baba, R. Noma, M. Kitano, J. N. Kondo, S. Hayashi, M. Hara, *J. Am. Chem. Soc.* **2011**, *133*, 4224 – 4227.
[14] L. Ye, S. Xie, B. Yue, L. Qian, S. Feng, S. C. Tsang, Y. Li, H. He, *CrystEngComm* **2010**, *12*, 344 – 347.
[15] J. Russell, J. Ness, M. Chopra, J. McMurray, W. E. Smith, *J. Pharm. Biomed. Anal.* **1994**, *12*, 863 – 866.
[16] J. Cenens, R. Schoonheydt, *Clays Clay Miner.* **1988**, *36*, 214 – 224.
[17] K. Tanabe, *Catal. Today* **2003**, *78*, 65 – 77.
[18] F. F. Brites, N. R. C. Fernandes-Machado, *Top. Catal.* **2011**, *54*, 264 – 269.
[19] E. R. Leite, C. Vila, J. Bettini, E. Longo, *J. Phys. Chem. B* **2006**, *110*, 18088 – 18090.